Glial Remodeling and Neural Plasticity in Human Retinal Detachment with Proliferative Vitreoretinopathy

Charanjit S. Sethi,[1] *Geoffrey P. Lewis,*[2] *Steven K. Fisher,*[2,3] *William P. Leitner,*[2] *Derrick L. Mann,*[2] *Philip J. Luthert,*[1] *and David G. Charteris*[1]

Purpose. To investigate glial remodeling and neuronal plasticity in adult human retinal detachment complicated by proliferative vitreoretinopathy (PVR) and to grade pathologic changes with a severity scoring system.

Methods. Sixteen full-thickness retinectomy specimens obtained at retinal relaxing surgery for PVR were fixed in 4% paraformaldehyde immediately after excision and compared to similarly processed normal donor retinas. Agarose-embedded sections (100-μm-thick) were double labeled for immunohistochemistry by confocal microscopy, with antibodies against rod opsin and GFAP; vimentin and M/L-cone opsin; calbindin D and S-cone opsin; and cytochrome oxidase and synaptophysin. These staining patterns formed the basis of a retinal pathology scoring system, and immunohistochemistry was also used to detect CD68, neurofilaments, protein kinase C, growth-associated protein-43, and a pan-cone–specific enzymatic marker. Morphology was also assessed by light microscopy of resin-embedded semithin sections.

Results. Prolonged detachment was characterized by photoreceptor degeneration and intracellular redistribution of opsin proteins to the plasma membrane in the outer nuclear layer (ONL). Remodeling of rod synaptic terminals was characterized by terminal retraction and also by axon extension to the inner retina in most specimens. Rod bipolar cell dendrites extended into the ONL, as did fine, horizontal cell processes. Large ganglion cells showed upregulated neurofilament and GAP-43 expression, with neurites sprouting from somata and axon collaterals. Anti-cytochrome oxidase labeling of surviving inner segments was reduced but detectable in all specimens, as was anti-calbindin D labeling of horizontal and amacrine cells. All specimens demonstrated a marked upregulation of Müller cell and astrocyte expression of GFAP and vimentin. More severe degenerative changes correlated with trauma and prolonged detachment duration when scored according to this system.

Conclusions. The neural and glial components of detached neurosensory retina complicated by PVR exhibit pathology that changes characteristically with increasing detachment severity. Even in advanced degeneration, most of the structural motifs necessary for functional recovery are retained. Evidence of remodeling in the first-, second-, and third-order neurons of detached adult human retina may represent an attempt to re-establish synaptic connectivity. (*Invest Ophthalmol Vis Sci.* 2005;46:329–342) DOI:10.1167/iovs.03-0518

Proliferative vitreoretinopathy (PVR) occurs in 5% to 10% of all rhegmatogenous retinal detachments (RRDs)[1] and is the most common cause of anatomic failure in RD surgery. PVR may be viewed as a maladapted wound-healing phenomenon[2] in which contractile periretinal cellular membranes can keep breaks open, create new ones, or distort retinal topography with visually detrimental sequelae.

In anterior PVR, intraretinal shortening may necessitate a full-thickness retinectomy to reattach the retina. Specimens of retinectomy tissue provide us with a glimpse of the cellular pathology occurring within and around chronically detached retina. Because many PVR cases are complicated, with histories of trauma or multiple vitreoretinal procedures,[3] only broad generalizations can be made about the spectrum of pathology encountered. Although the histologic and ultrastructural features of human PVR have been well described, most of these studies have focused on characterizing components of periretinal membranes. Intraretinal changes that adversely affect visual recovery have yet to be characterized comprehensively in human tissue, although from experimental data, we might infer that both neuronal remodeling and intraretinal gliosis could interfere with the maintenance or restoration of functional synapses after detachment.[4,5] In this study, we used laser scanning confocal microscopy with a well-characterized panel of antibodies to determine characteristic features in the response of neuronal and non-neuronal retinal cell types in human RD complicated by PVR. This approach has also enabled us to derive a simple pathology scoring system.

It is important to establish a detailed description of the pathology of human PVR. These data will enable more critical appraisal of animal models for clinical relevance and may play a role in the evaluation of retinal biopsy material obtained in clinical treatment trials. Part of this work has been presented and published in abstract form (Charteris DG, et al. *IOVS* 2000;41:ARVO Abstract 664; and Sethi CS, et al. *IOVS* 2001; 31:ARVO Abstract 445).

Materials and Methods

Patients

Table 1 illustrates the range of conditions for which surgery was undertaken in obtaining specimens for this study. The number of procedures refers to vitreoretinal operations only, up to and including the surgery at which the specimen was obtained. The estimated total

From the [1]Moorfields Eye Hospital and the Institute of Ophthalmology, University College London, London, United Kingdom; and the [2]Neuroscience Research Institute and the [3]Department of Molecular, Cellular, and Developmental Biology, University of California, Santa Barbara, California.

Supported by Grant G84/5452 from the Medical Research Council, United Kingdom; Grant EY-00888 from the National Eye Institute; the Special Trustees of Moorfields Eye Hospital; The Royal College of Surgeons of Edinburgh; the Royal Blind Asylum/Scottish National Institution for the War Blinded; a Bogue Travel Fellowship, University College London; the University of London Central Research Fund; and the Pathological Society of Great Britain and Ireland. CSS is a Medical Research Council Clinical Training Fellow (Grant G84/5452).

Submitted for publication May 24, 2003; revised October 24, 2003, and April 30, 2004; accepted May 7, 2004.

Disclosure: **C.S. Sethi**, None; **G.P. Lewis**, None; **S.K. Fisher**, None; **W.P. Leitner**, None; **D.L. Mann**, None; **P.J. Luthert**, None; **D.G. Charteris**, None

The publication costs of this article were defrayed in part by page charge payment. This article must therefore be marked "*advertisement*" in accordance with 18 U.S.C. §1734 solely to indicate this fact.

Corresponding author: Charanjit S. Sethi, Departments of Pathology and Cell Biology, Institute of Ophthalmology, 11-43 Bath Street, London EC1V 9EL, UK; cj@csethi.com.

TABLE 1. Clinical Details

Age/Sex	Aetiology of Retinal Detachment	Prior Procedures (*n*)	RD Duration (Total)	Prior Silicone Oil	RD/PVR at Surgery
17M	Trauma, penetrating injury with VH	4	7 months	No	Inferior and subretinal PVR
58F	RRD, superior tear in lattice plus VH	1	3 months	No	Total RD (CP12)
60M	RRD with VH in pseudophake	2	5 months	Yes (1 month)	Inferior and anterior PVR (CA8/CP8)
21M	Trauma, blunt, globe rupture, VH.	4	2 months	Yes (2 months)	Inferior and subretinal PVR
62M	RRD in myope with lattice	3	3 months	Yes (2 months)	Inferior and anterior PVR
76M	Trauma, blunt with VH	1	4 months	Yes (3 months)	Inferior, anterior, subretinal PVR
15F	RRD in patient with ROP	5	6 months	Yes (6 months)	CA12
27M	RRD in pseudophake (congenital cataract)	4	3 months	Yes (3 months)	Inferior and subretinal PVR
48M	RRD	4	2 months	Yes (2 months)	Inferior star folds (CA4)
76F	RRD in pseudophake	3	2 months	No	Inferior (CA8)
55M	RRD in myope	3	3 weeks	No	Inferior (CA6)
32M	Trauma, penetrating injury with VH	1	1 month	No	CP8
21M	Acute retinal necrosis	2	1.5 months	Yes (3 months)	Inferior PVR
13M	Trauma, blunt	4	1.5 months	Yes (4 months)	Total RD (CA5 CP12)
28M	Trauma, penetrating	4	2 months	Yes (7 months)	Inferior and subretinal PVR
25F	Trauma, penetrating injury	5	2 months	Yes (2 months)	Total RD (CA5 CP8)

VH, vitreous haemorrhage; RRD, rhegmatogenous retinal detachment; ROP, retinopathy of prematurity.

duration of RD was obtained by accumulating suspected periods of RD before the retinectomy from each patient's clinical record. PVR classification, where recorded in the clinical notes, was made according to the Retina Society's grading. All surgery was conducted at Moorfields Eye Hospital by consultant vitreoretinal surgeons or senior fellows. The study protocol was in accordance with the provisions of the Declaration of Helsinki for research involving human subjects and human tissue. All patients provided informed consent for the use of retinal tissue excised during surgery and the study was approved by the Ethics Committee of Moorfields Eye Hospital.

Immunohistochemistry

Retinectomy specimens from the 16 patients were removed from the globe after excision and immediately fixed in 4% paraformaldehyde in sodium cacodylate buffer (0.1 M; [pH 7.4]; Electron Microscopy Sciences, Fort Washington, PA) for a minimum of 24 hours. Control tissue was used from a 79-year-old female donor. Peripheral retina from an anatomic location similar to the retinectomy specimens was used for analysis. After they were rinsed in PBS, the specimens were orientated in 5% agarose (Sigma-Aldrich, St. Louis, MO) in PBS. Sections (100-μm-thick) were cut with a vibratome (Technical Products International, Polysciences, Warrington, PA) and incubated in normal donkey serum (1:20; Jackson ImmunoResearch, West Grove, PA) in PBS containing 0.5% bovine serum albumin (BSA; Fisher Scientific, Pittsburgh, PA), 0.1% Triton X-100 (Roche Molecular Biochemicals, Indianapolis, IN), and 0.1% sodium azide (Sigma-Aldrich) overnight at 4°C on a rotator (PBS, BSA, Triton X-100, and azide is referred to as PBTA). After the removal of blocking serum, primary antibodies were added in four sets of pairs: anti-glial fibrillary acidic protein (GFAP; 1:500; Dako, Carpinteria, CA) with anti-rod opsin (1:50; gift from Robert Molday, University of British Columbia, Vancouver, BC, Canada); anti-vimentin (1:500; Dako) with anti-medium to long-wavelength (M/L) cone opsin (1:2000; gift from Jeremy Nathans, Johns Hopkins University School of Medicine, Baltimore, MD); anti-calbindin D (1:1000; Sigma) with anti-short-wavelength (S) cone opsin (1:2000; gift from Jeremy Nathans); and anti-cytochrome oxidase (CO; 1 μg/mL; Molecular Probes, Eugene, OR) with anti-synaptophysin (1:100; Dako). Additional antibodies were used to detect CD68 (1:200; Dako), neurofilaments (1:500; Biomeda Corp., Foster City, CA); protein kinase C (PKC; 1/100: Biomol Research Laboratories Inc., Plymouth Meeting, PA); growth-associated protein (GAP)-43 (1/200: Chemicon International, Temecula, CA) and cones, regardless of spectral sensitivity (7G6 culture supernatant, mouse monoclonal antibody used 1/100; gift from Peter MacLeish, Morehouse School of Medicine, Atlanta, GA).

After overnight incubation at 4°C on a rotator, sections were rinsed in PBTA and incubated again overnight at 4°C with the secondary antibody. Donkey anti-mouse and donkey anti-rabbit secondary antibodies were used for each combination of primary antibodies, conjugated to Cy2 or Cy3 (Jackson ImmunoResearch). All secondary antibodies were used at a dilution of 1:200, and all antibodies were diluted in PBTA. Selected sections were counterstained with DAPI (1:5000; Dako) for 5 minutes in one of the final washes. The sections were then rinsed, mounted in *N*-propyl gallate in glycerol and viewed on a laser scanning confocal microscope (model 1024; Bio-Rad, Hercules CA, or LSM 510, Carl Zeiss Meditec, Oberkochen, Germany).

The proportion of rod photoreceptors with obvious outer and inner segment material, and hence most capable of regeneration after reattachment, was calculated by averaging cell counts from two independent regions of each specimen.

Apoptosis Assay

Apoptotic cells were detected in 100-μm-thick vibratome-cut sections using a kit (In Situ Cell Death Detection; Roche Molecular Biochemicals), which employs a TUNEL reaction to detect apoptosis at the single-cell level in tissues. Tissue from a 3-day detached feline retina was used as a positive control, as this is an established time point for maximum cell death by apoptosis after experimental RD.[6]

Light Microscopy

Where a sufficiently large specimen had been obtained, it was divided, and half was prepared for morphologic analysis by light microscopy, by fixation in 1% paraformaldehyde and 1% glutaraldehyde (Electron Microscopy Sciences) in sodium phosphate buffer (PBS; 0.086 M, pH 7.3) overnight at 4°C. The tissue was then fixed in 2% osmium tetroxide in phosphate buffer for 1 hour, dehydrated in increasing concentrations of ethanol, and embedded in Spurr's resin (Polysciences). Specimens were sectioned at 1 μm and counterstained with saturated aqueous *p*-phenyldiamine (PPDA) or toluidine blue.

Immunocytochemical staining of etched semithin sections was performed according to the method of Pow and Robinson.[7] Briefly, semithin sections dried onto 10-well slides were etched for 5 minutes with 11% sodium ethoxide, rinsed with distilled water, and blocked with 1% BSA in PBS (PBS-BSA). After three rinses in PBS, sections were incubated overnight in rabbit anti-GFAP (1:500; Dako) diluted in PBS-BSA. Sections were then rinsed with PBS, and incubated for 3 hours at room temperature with biotinylated swine anti-rabbit/goat/mouse/rabbit multi-link (1:150; Dako) diluted in PBS-BSA, rinsed in PBS, and

incubated for a further 3 hours in streptavidin avidin-biotin complex (ABC)/horseradish peroxidase (Dako). After thorough rinsing in PBS, chromogen was visualized by immersion for 1 to 2 minutes in a solution of 3′3′ diaminobenzidine (0.6 mg/mL) containing 0.003% hydrogen peroxide and buffered to pH 7.4 with 0.05 M Tris-HCl buffer. Finally, sections were rinsed, dried, stained with 1% alcoholic toluidine blue and mounted for light microscopy.

Results

Light Microscopy

Figure 1 demonstrates a semithin etched section of a full-thickness retinectomy specimen labeled with anti-GFAP (dark green) and a toluidine blue counterstain. Residual rod outer segment (OS; thin, slender) and cone inner segment (IS; bulbous, speckled) material were visible sclerad to the prominently stained outer limiting membrane (OLM). Hypertrophied trunks of reactive Müller cells disrupted the outer (ONL) and inner (INL) nuclear layers, and there was also an area of lateral Müller cell branching in the inner plexiform layer (IPL; double-headed arrow). A normal-looking rounded Müller cell body with prominent nucleolus was present at the vitread border of the INL (block arrow). Other Müller cell nuclei had been translocated into the mid-INL and ONL (arrowheads). There are examples of cone cell bodies withdrawn from the OLM (arrow) into the ONL. Reactive Müller cells around a large inner retinal blood vessel had breached the inner limiting membrane to form an incipient epiretinal membrane (ERM).

Immunohistochemistry

All specimens demonstrated significant photoreceptor degeneration. Figure 2 depicts the results from four antibody pairs. A spectrum of degenerative changes, described as mild (Figs. 2B, 2F, 2J, 2N), moderate (Figs. 2C, 2G, 2K, 2O), or severe (Figs. 2D, 2H, 2L, 2P) was compared to normal staining patterns (Figs. 2A, 2E, 2I, 2M) in donor retinal tissue.

Photoreceptor Proteins. In normal retina (Fig 2A), anti-rod opsin labeled rod OS. The proportion of rod photoreceptors with obvious OS and IS was estimated to be <25% of the cell count in normal retina in 5 of the 16 specimens, 25% to 50% in 3 of 16, 50% to 75% in 3 of 16, and >75% in 5 of 16. After RD, the OS were disorganized, and rod opsin was detected in the plasma membrane of the IS and in many cases throughout the plasma membrane of the cell. In less severe degeneration, this was manifest as positive labeling around occasional cell bodies in the ONL (Fig. 2B), but in more advanced degeneration, anti-rod opsin labeling was detected around virtually all rod photoreceptor cell bodies in the ONL (Fig. 2C) and in the plasma membrane of beaded neurites extending toward the inner retina (Figs. 2D, 5A, arrows). Double-labeling with anti-rod opsin and anti-synaptophysin demonstrated that some of these extended neurites contained synaptic vesicle protein in their beaded varicosities (Fig. 5B). In more advanced degeneration (Fig. 2D), photoreceptor cell death resulted in reduced anti-rod opsin labeling in the ONL, though extending neurites were still visible in most cases (14/16 specimens; Fig. 2D, arrows).

Anti-M/L-cone opsin localized to a subset of cone OS in normal retina (Fig. 2E) and these are reduced in length after detachment (Fig. 2F). With more advanced degeneration, only truncated caps of outer segment material were detected, with subtle redistribution of opsin protein to the plasma membrane of swollen IS (Fig. 2G, arrow) and occasional cell bodies. Severe degeneration was associated with absence of M/L-cone opsin labeling (2/16 specimens).

S cones responded in a manner similar to the response of M/L cones, with reduction in OS length (Fig. 2J) followed by more marked truncation and redistribution of opsin labeling to the plasma membrane of the IS (Fig. 2K, arrow). Once the outer segment was lost completely, some S cones demonstrated opsin protein redistribution to the plasma membrane surrounding the remaining IS, cell body, and synaptic terminal (Fig. 2L). Anti-M/L-cone opsin labeling seldom delineated cells as clearly as the anti-S-cone opsin labeling depicted in Fig. 2L. In more advanced degeneration, no anti-S cone labeling was detected (6/16 specimens).

The anti-cone monoclonal antibody 7G6 demonstrated significantly more cones than were detected by anti-opsin staining alone (Fig. 3A). This antibody labeled entire cells from the remaining OS to the synaptic terminal, many of which assume a flattened morphology compared to normal retina (Fig. 3A, arrows). Double-labeling with anti-7G6 and anti-M/L-cone opsin antibodies clearly identified OS belonging to M/L cones

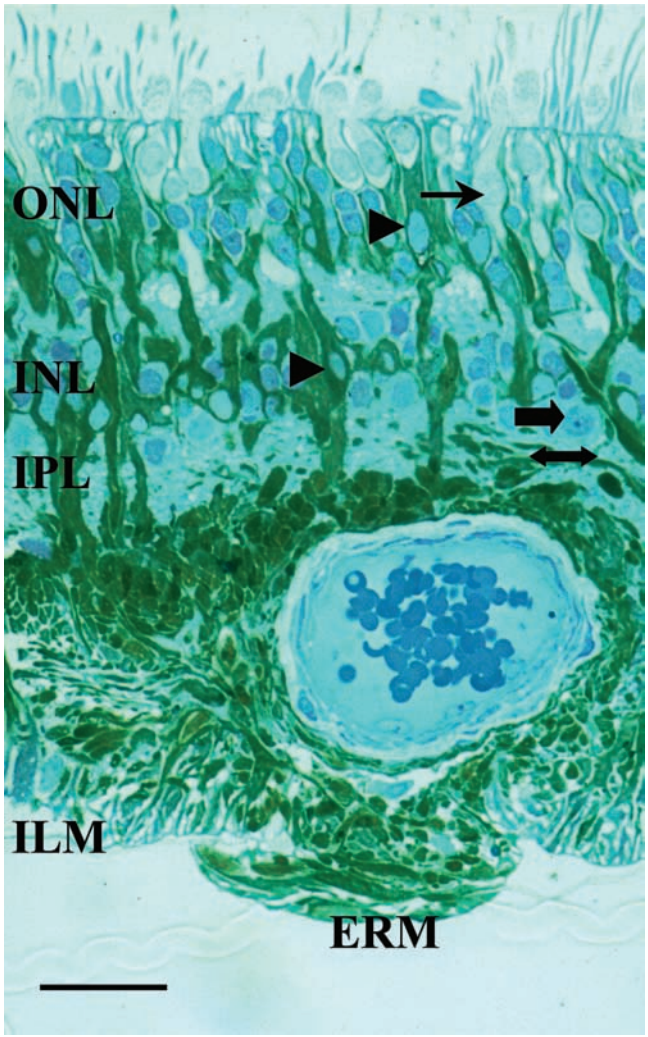

Figure 1. Semithin human retinal section obtained during retinectomy, etched, labeled with anti-GFAP (*green*) and counterstained with toluidine blue. Residual IS and OS can be seen at the *top* of the micrograph. The ONL and INL are disrupted by hypertrophied trunks of reactive Müller cells containing GFAP. *Double-headed arrow*: area of lateral Müller cell branching in the IPL. *Block arrow*: normal-looking, rounded Müller cell body with prominent nucleolus, at the vitread border of the INL. *Arrowheads*: other Müller cell nuclei have been translocated into the mid-INL and -ONL. *Arrow*: cone cell body withdrawn from the OLM. Reactive Müller cells around a large inner retinal blood vessel have breached the ILM to form an incipient ERM. Scale bar, 50 μm.

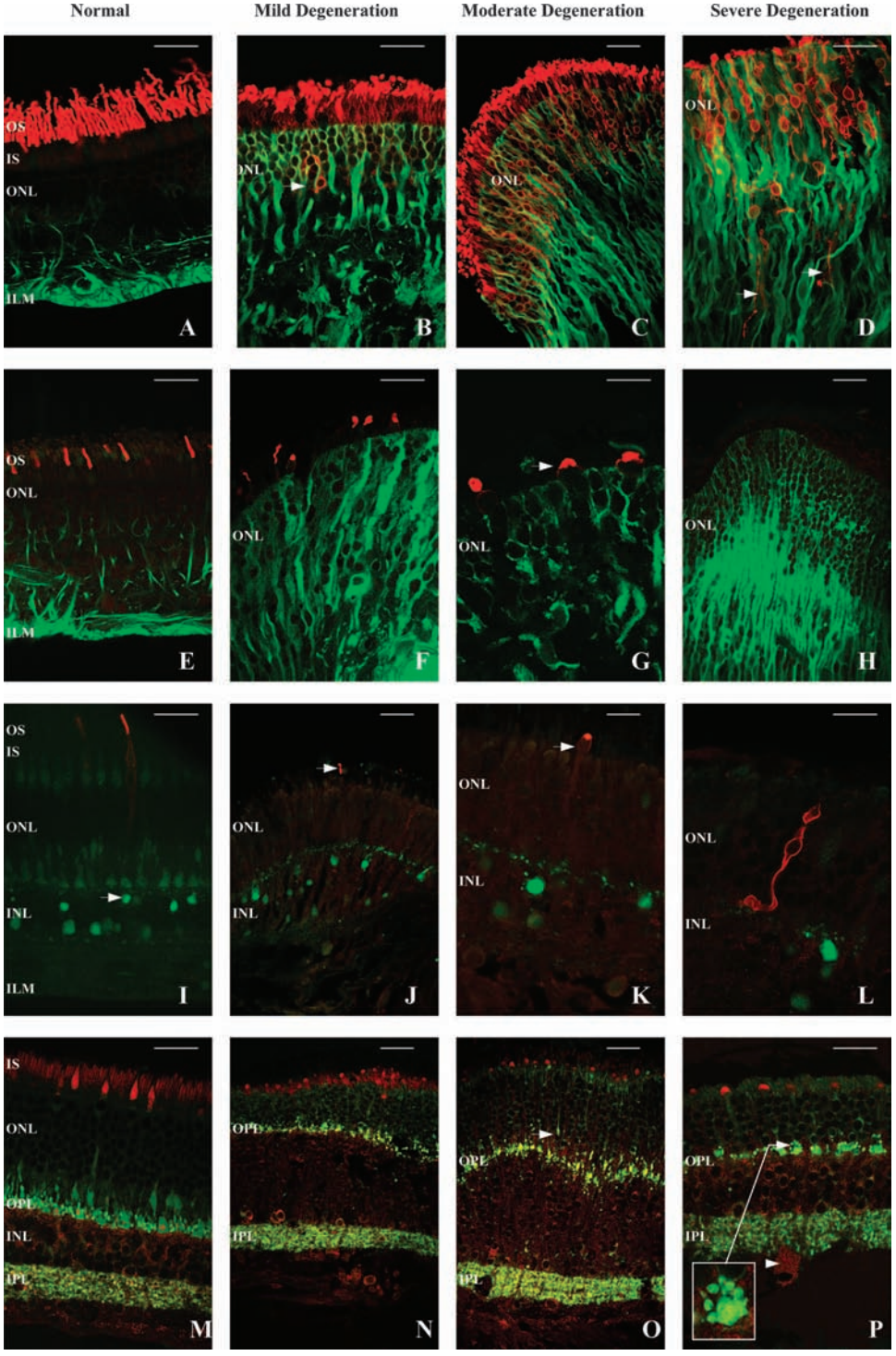

FIGURE 2. Double-labeled immunohistochemistry using antibodies to GFAP and rod opsin (**A–D**); vimentin and M/L-cone opsin (**E–H**); calbindin D and S-cone opsin (**I–L**); and cytochrome oxidase (CO) and synaptophysin (**M–P**). Comparisons were made between normal donor retina (**A**, **E**, **I**, **M**) and degenerative changes in the retinectomy specimens described as mild (**B**, **F**, **J**, **N**), moderate (**C**, **G**, **K**, **O**), and severe (**D**, **H**, **L**, **P**). (**A–D**) Anti-GFAP (*green*); anti-rod opsin (*red*). In normal retina, GFAP was mainly restricted to the end feet region of Müller cells in the inner retina, though some label was detected up to the ONL (**A**). Rod opsin was localized to the photoreceptor OS. After detachment, GFAP increased throughout the entire Müller cell to the OLM. As OS degeneration began after detachment, rod opsin labeling was more intense in the plasma membrane of the IS and cell body, initially manifesting as positive labeling around occasional cell bodies in the ONL (**B**, *arrow*), but as photoreceptor degeneration progressed, anti-rod opsin labeling was detected around virtually all rod photoreceptor cell bodies in the ONL (**C**). In more advanced degeneration (**D**), photoreceptor cell death resulted in reduced anti-rod opsin labeling in the ONL, though it was detectable in the plasma membrane of beaded neurites extending toward the inner retina (*arrows*). (**E–H**) Anti-vimentin (*green*); anti-M/L-cone opsin (*red*). In normal retina, vimentin was mainly restricted to the inner portion of the Müller cells, though some label was detected up to the ONL, and M/L-cone opsin was restricted to the cone OS (**E**). After detachment, vimentin was upregulated across the entire Müller cell in a manner similar to GFAP and the OS of M/L cones were reduced in length (**F**). With more advanced degeneration, only truncated caps of OS were detected, with subtle redistribution of opsin protein to the plasma membrane of swollen IS (**G**, *arrow*) and occasional cell bodies. Severe degeneration was associated with absence of anti-M/L-cone opsin labeling (**H**; 2/16 specimens). (**I–L**) Anti-calbindin D (*green*); anti-S cone opsin (*red*). In normal retina, anti-calbindin D labeled cones and cells in the INL (**I**). Cells staining brightly in the outermost stratum of the INL were probably horizontal cells (*arrow*), whereas larger cells in the innermost stratum were probably amacrine cells. On detachment, cone labeling was gradually lost, and there were progressively fewer labeled cells in the INL (**J–L**). S-cone opsin was localized to the OS in normal retina—the faint labeling of plasma membrane around more proximal cell compartments in this control sample is probably a fixation artifact. S cones respond similarly to M/L cones on detachment, with initial reduction in OS length (**J**, *arrow*) followed by more marked truncation and redistribution to the plasma membrane of the inner segment (**K**, *arrow*). Once the OS has been lost completely, some S cones demonstrate opsin protein redistribution to the plasma membrane surrounding the remaining inner segment, cell body and synaptic terminal (**L**). In more advanced degeneration, no anti-S cone labeling was detected (6/16 specimens). (**M–P**) Anti-CO (*red*); anti-synaptophysin (*green*). In normal retina, CO was detected most strongly in the photoreceptor IS. After RD, the IS became less ordered (**N**) and the level of labeling in the photoreceptor layer decreased, eventually being only apparent in truncated IS of surviving cones (**O**, **P**). Some mitochondrial activity was detectable within large ganglion cells, even in advanced degeneration (**P**, *arrowhead*). Synaptophysin was normally located in the photoreceptor terminals of the OPL and synaptic vesicles in the IPL (**M**, the faint staining seen in the ONL is probably a fixation artifact). After detachment, the IPL staining was initially preserved (**N**, **O**) but declined in more advanced degeneration (**P**). Retraction and degeneration of rod synaptic terminals was an early feature of RD (**O**, *arrowhead*), and, as this process continued, the OPL assumed an expanded and less compact appearance from anti-synaptophysin labeling of retracting photoreceptor axons and synaptophysin redistribution around cell bodies in the ONL. With advancing photoreceptor loss, the OPL became thin, and surviving rod terminals tended to be clustered around cone pedicles (**P**, *arrow* and shown in higher magnification in the *inset*). Scale bar: (**G**, **K**, **L**) 25 μm; (**A–F**, **H–J**, **M–P**) 50 μm.

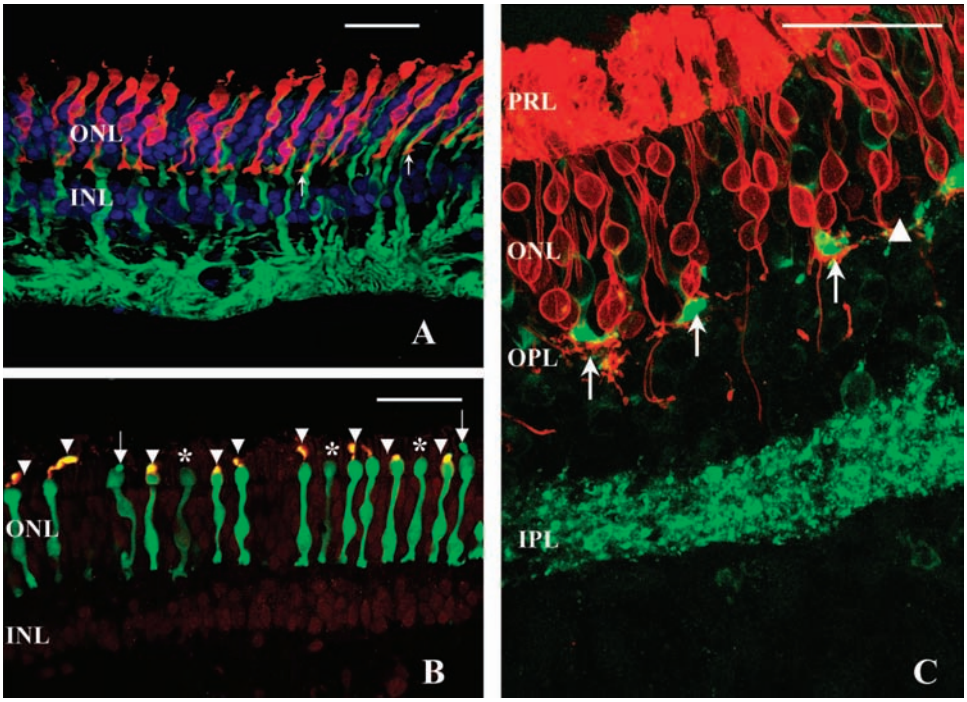

FIGURE 3. Confocal images of retinectomy sections to demonstrate cone morphology and possible rod–cone interaction in RD with PVR. (**A**) Anti-7G6 (*red*); anti-GFAP (*green*); DAPI nuclear counterstain (*blue*). The cones were clearly labeled with anti-7G6. Some of the cell bodies were withdrawn into the ONL and some of the synaptic terminals have assumed a flattened morphology (*arrows*). Hypertrophied Müller cell processes extended across the entire retina to the OLM. (**B**) Anti-7G6 (*green*); anti-M/L cone opsin (*red*). All cones were clearly labeled with anti-7G6, and colabeling with anti-M/L cone opsin identified the OS of M/L cones (*yellow*; *arrowheads*). Green outer segments probably represent S cones (*arrows*), whereas cones that had no discernible OS may have been either class of cone, no longer producing opsin protein after RD. (**C**) Anti-rod opsin (*red*); anti-synaptophysin (*green*). Surviving rod OS and IS were visible in the photoreceptor layer (PRL) with redistribution of rod opsin to cell bodies in the ONL. Anti-synaptophysin labeled cone pedicles prominently in the OPL, outlining the cell bodies of some cones in the ONL and labeling processes in the IPL. Some of the rod cell bodies extended axons past the OPL toward the inner retina, and there appeared to be a clustering of rod terminals around surviving cone pedicles in the OPL (*arrows*). Where a cone pedicle appeared to have been lost (*arrowhead*), the clustering phenomenon was not seen. Scale bar, 50 μm.

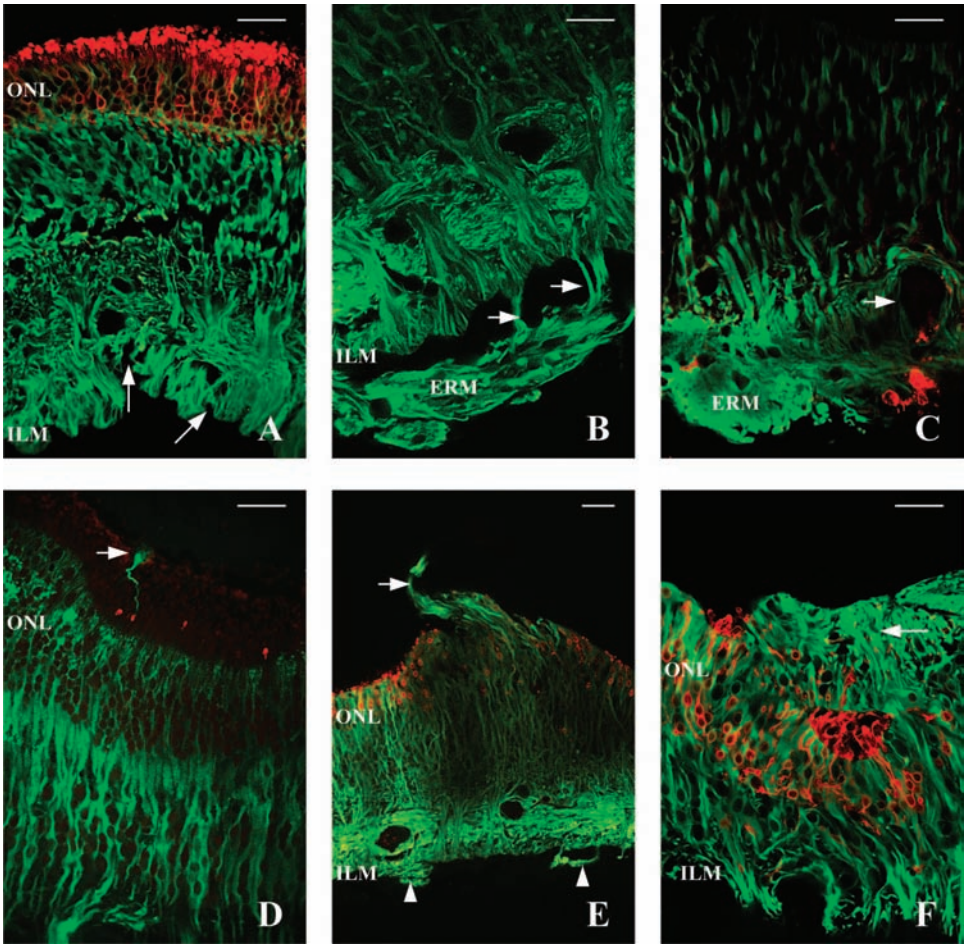

FIGURE 4. Epiretinal (**A–C**) and subretinal (**D–F**) glial remodeling in human RD. (**A**) Anti-GFAP (*green*); anti-rod opsin (*red*). Wrinkling of the internal limiting membrane (*arrows*), an early feature occurring after upregulation of intermediate filaments in the Müller cells. (**B**) Anti-GFAP (*green*). An ERM connected to the retina by glial pegs (*arrows*). (**C**) Anti-GFAP (*green*); anti-CD68 (*red*). An example of early ERM formation near an inner retinal blood vessel (*arrow*), from which macrophages appeared to be extravasating. (**D**) Anti-vimentin (*green*); anti-M/L cone opsin (*red*). A focal Müller cell extension (*arrow*) into the subretinal space, in proximity to the truncated OS of a surviving M/L cone. (**E**, **F**) Anti-GFAP (*green*); anti-rod opsin (*red*). Examples of subretinal gliosis (*arrows*), with additional foci of incipient epiretinal proliferation (**E**, *arrowheads*). Note the almost complete loss of OS and IS in the areas underlying the multilayered gliotic membranes and significantly reduced labeling for rod opsin in the plasma membrane around cell bodies in the ONL (**F**). Some photoreceptor nuclei were incorporated into the subretinal scars. Scale bars, 50 μm.

(Fig. 3B, yellow, arrowheads) and S cones (Fig. 3B, green, arrows). A third population of cones detected by anti-7G6 labeling had no demonstrable OS (Fig. 3B, asterisks) and could thus represent cone photoreceptors of either spectral sensitivity that were no longer producing opsin protein. This suggests that failure to detect cone opsin by immunohistochemical means does not equate to absence of potentially viable cone cells within a specimen.

Intermediate Filaments and Periretinal Membranes. In normal retina, anti-GFAP and anti-vimentin predominantly labeled inner retinal astrocytes and Müller cell foot processes (Figs. 2A, 2E). Vimentin was detected up to the ONL in elderly subjects, as seen in this control specimen (Fig. 2E). All retinectomy specimens demonstrated GFAP (Figs. 2B–D) and vimentin (Figs. 2F–H) labeling across the entire Müller cell to the OLM. In severe degeneration, the glial component of the retina was significantly expanded, filling areas previously occupied by degenerated retinal neurons (Figs. 2D, 2H). Wrinkling of the inner limiting membrane (ILM) was also a common feature (Fig. 4A, arrows).

ERM components labeling for intermediate filament proteins were visible in 9 of 16 specimens and subretinal gliosis in 11of 16. Mature ERMs were multilayered in appearance and predominantly glial in origin, derived from intraretinal Müller cells that extended peg-like connections to more confluent epiretinal gliosis (Fig. 4B, arrows). Often, breaches in the ILM giving rise to epiretinal glial hypertrophy arose near or directly vitread to large blood vessels in the inner retina (Fig. 4C, arrow). Focal glial breaches of the OLM did not appear to compromise the integrity of adjacent photoreceptors (Fig. 4D), whereas confluent, multilayered glial proliferation in the subretinal space resulted in significant photoreceptor disruption (Figs. 4E, 4F, arrows).

Second-Order Neurons. In normal retina, anti-calbindin D labeled cones and cells in the INL (Fig. 2I). Cells staining brightly in the outermost stratum of the INL were likely to be horizontal cells (Fig. 2I, arrow), whereas larger cells in the innermost stratum were likely to be amacrine cells. It is not possible to be certain of the precise phenotype of a given cell without using more specific antibodies. On detachment, cone labeling was gradually lost. Good cone labeling was present in only 3 of 16 specimens. Faint labeling was visible in 4 of 16, and, in the remaining 9 specimens, labeling was absent. In a few specimens, anti-calbindin D–labeled processes extended from the outer stratum of the INL, presumably from horizontal cell somata, to well within the ONL (Fig. 5E, arrows). No such processes were detected in normal retina.

Anti-PKC labeling was used to visualize rod bipolar cells and, in normal retina, labeled a well-ordered layer of rod bipolar cell bodies in the INL (Fig. 5C). In the example shown, taken from an elderly normal subject, there were also some PKC-labeled rod bipolar cell neurite extensions into the ONL, though these were absent in control tissue from younger donors, where synaptic contacts in the outer plexiform layer (OPL) marked the outer limit of anti-PKC labeling (data not shown). Retinectomy specimens demonstrated disruption of rod bipolar cell body stratification and numerous villiform extensions of neurites into the ONL (Fig. 5D). In advanced degeneration, these extensions were either absent or their protein content or caliber was below the threshold of detection using our methods.

Third-Order Neurons. In normal retina, anti-neurofilament labeling was present in axons of the nerve fiber layer and faint speckled labeling in the IPL (data not shown). Both patterns were retained in retinectomy specimens, though the IPL labeling was reduced. In addition, large ganglion cell bodies with accumulated neurofilaments were visible in retinectomy tissue (Fig. 5G, red). Where ERM formation was observed, anti-neurofilament–labeled processes extended from the somata of these cells and nearby axons into epiretinal glial tissue, following the path taken by Müller cells breaching the ILM (Fig. 5F, arrow). This observation was reinforced by the identification of anti-neurofilament–labeled processes in ERM tissue peeled away during PVR surgery, an example of which is shown in Fig. 5H.

Anti-GAP-43 identifies the cell bodies of injured or regenerating neurons[8] and in normal retina was confined to a trilaminar labeling pattern in the IPL (Fig. 5J). Some of the large ganglion cells identified in retinectomy specimens were also labeled with anti-GAP-43, and the IPL labeling was less ordered and reduced in intensity (Fig. 5I).

Cytochrome Oxidase. In normal retina, anti-cytochrome oxidase identified mitochondria and labeled the IS of photoreceptors strongly (Fig. 2M). As degeneration began after RD, the IS became less ordered (Fig. 2N), and the level of labeling in the photoreceptor layer lessened and eventually was apparent only in truncated IS of surviving cones (Figs. 2O, 2P). Some mitochondrial activity was still detectable within large ganglion cells, an example of which is depicted in Figure 2P abutting the IPL (arrowhead).

Synaptophysin. Synaptic vesicle protein identified by anti-synaptophysin is normally located in well-ordered OPL and IPL strata (Fig. 2M). After detachment, the intensity of IPL staining was initially preserved (Figs. 2N, 2O) but declined in more advanced disease (Fig. 2P). Retraction and degeneration of rod synaptic terminals is an early feature of experimental RD.[5] As this process occurs in the human detachments, the OPL assumes an expanded and less compact appearance demonstrated by anti-synaptophysin labeling of these retracted terminals (Fig. 2O, arrow) and photoreceptor axons extending to the inner retina. Double labeling with anti-rod opsin and anti-synaptophysin (Fig. 5B) suggests that some of the vesicular staining in the INL represents synaptic vesicle protein in extended rod neurites. With advancing photoreceptor loss, the OPL became thin, and surviving rod terminals tended to be clustered around cone pedicles (Fig. 2P, arrow and shown at higher magnification in the inset; Fig 3C, arrows).

Apoptosis

Very few apoptotic cells were noted with the methods we used to examine the tissue, even in specimens with severe degenerative features, suggesting that the maximum period of apoptotic cell death had passed before the specimen was obtained.

Retinal Pathology Scores

Subcellular changes in labeling patterns for anti-rod opsin, anti-M/L-cone opsin, anti-S-cone opsin, anti-calbindin D, anti-cytochrome oxidase, and anti-synaptophysin were graded as mild, moderate, or severe, as illustrated in Figure 2 and tabulated in Table 2. More advanced disease was associated with a higher score, and, as none of the specimens demonstrated an entirely normal pattern of staining, this gave a combined score between 6 and 18 for this panel of antibodies.

Intermediate filament staining was graded independently for anti-GFAP and anti-vimentin labeling. Although superficially this may appear to overscore the contribution of glial cells to the final total, we found that periretinal disease was occasionally detected by only one of these labels because of sampling variation, and so we felt justified in using information from both antibodies to derive the score. The intermediate filament staining was graded in a cumulative manner, with all specimens receiving a minimum score of +1, signifying upregulation of intermediate filament staining to the OLM in all cases. A focal breach of the ILM (Fig. 4E, arrowhead) or OLM (Fig. 4D, arrow) scored an additional point, and if any of these breaches

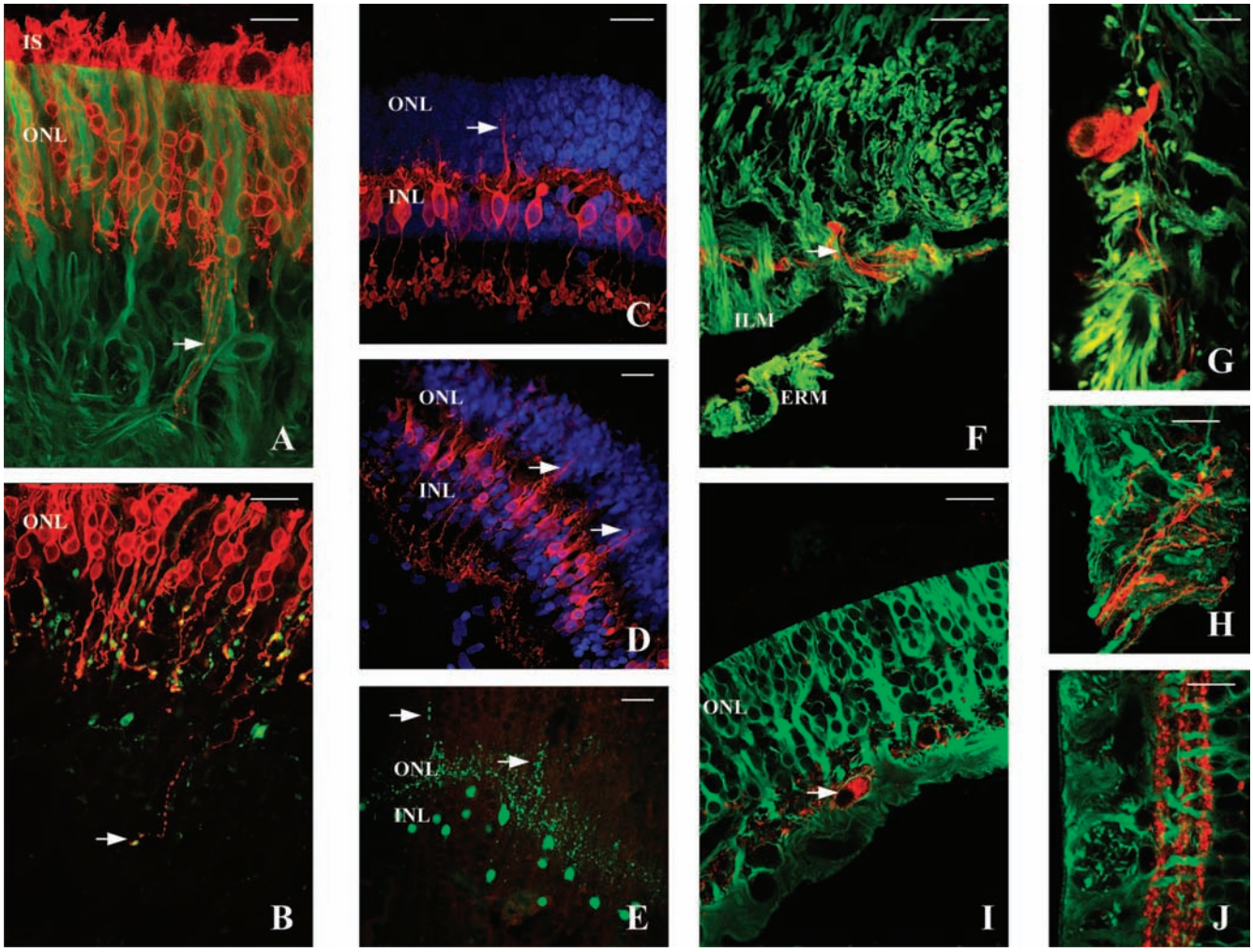

FIGURE 5. Remodeling events in (**A**, **B**) first-, (**C**–**E**) second-, and (**F**–**J**) third-order retinal neurons. (**A**) Anti-rod opsin (*red*); anti-GFAP (*green*). Beaded neurites extended along Müller cell arcades toward the inner retina (*arrow*). Double labeling with anti-rod opsin and anti-synaptophysin (**B**) demonstrated that some of the varicosities in these processes contained synaptic vesicle protein (*arrow*, *yellow*). In normal, aged donor retina (**C**) and retinectomy specimens (**D**), rod bipolar cells were labeled with anti-protein kinase C (*red*) and DAPI (*blue*) used as a nuclear counterstain. Normal retina (**C**) has an orderly arrangement of rod bipolar cell nuclei in the INL, with occasional fine dendrites extending into the ONL (*arrow*). The stratification of rod bipolar cell somata was less ordered in the retinectomy specimens (**D**) and villiform extensions (*arrows*) into the ONL were a frequent feature of specimens with moderate to severe photoreceptor degeneration. Anti-calbindin D labeling (**E**, *green*) also demonstrated fine extensions from horizontal cells into the ONL (*arrows*). (**F**–**H**) Anti-neurofilament (*red*); anti-GFAP (*green*). In retinectomy specimens, but not normal donor retina, large ganglion cell bodies contain neurofilaments (**G**). Where ERMs were detected, axon-like processes were seen to extend into the gliotic regions with Müller cell processes (**F**, *arrow*). Analysis of excised ERM tissue also consistently demonstrated the presence of these processes (**H**). (**I**, **J**) Anti-GAP-43 (*red*); anti-GFAP (*green*). Some of the larger ganglion cells in retinectomy specimens also demonstrated positive labeling for anti-GAP-43 (**I**, *arrow*), though the ordered trilaminar staining pattern for anti-GAP-43 in normal donor retina (**J**) was much less apparent in detachment retinal tissue. Scale bar: 50 μm except in (**G**) 15 μm; (**J**) 25 μm.

progressed to multilayered epiretinal (Fig. 4B) or subretinal (Figs. 4E, 4F, arrows) gliosis, an additional point was added. Thus, a specimen with anti-GFAP labeling across the entire Müller cell (+1), multilayered ERM (+2), and multilayered subretinal gliosis (+2) would score a maximum of +5 for this antibody. Application of these criteria to anti-vimentin labeling gave a combined total score between 2 and 10 for these antibodies.

Finally, an additional point was added to the score if we observed significant wrinkling of the ILM, signifying contraction in the inner retina, and a further point was added in the presence of rod axon extensions, signifying remodeling of first-order neuron synapses in the context of outer segment degeneration. The total retinal pathology score was thus between 6 and 30.

The prevalence of specific immunohistochemical and morphological observations in our specimens has been summarized in Table 3.

DISCUSSION

Early and complete retinal reattachment remains the best preventive measure against the subsequent development of PVR. Recent work in a well-characterized feline model of RD demonstrates that rapid retinal reattachment may retard and even reverse some of the cellular and molecular changes initiated by RD.[9] Despite some progress in the adjuvant treatment of patients at high risk of PVR,[10–12] management of established or recurrent disease remains a significant problem in vitreoretinal surgery. A review of published series between 1992 and 2000

TABLE 2. Retinal Pathology Scoring System

Antibody to:	Normal	Mild (+1)	Moderate (+2)	Severe (+3)
Rod opsin	Localized to rod outer segments (OS)	OS length decreased and redistribution to inner segments (IS) +/− occasional cell body in ONL	OS more degenerate but still detectable with redistribution to most cell bodies in ONL	OS lost, degenerated IS with cell death leading to patchy staining of ONL
M/L cone Opsin	Localized to OS	OS length decreased with redistribution to IS	Further OS truncation (residual caps of OS material on swollen IS) with redistribution to entire cell in places	No OS, some residual plasma membrane staining of IS or entire cell
S cone opsin	Localized to OS	OS essentially preserved with redistribution to IS	Reduced OS length (residual caps of OS material on swollen IS) with redistribution to entire cell in places	No OS, some residual plasma membrane staining of IS or entire cell
Calbindin O	Good staining of horizontal cells (HCs) and amacrine cells (ACs) and labeling of cones	Reasonable labeling of cells in INL, though reduced number and intensity compared with normal; some cone staining retained	Further reduction in number and staining intensity of cells in INL with loss of cone labeling (occasionally some HC processes extending into ONL)	Only occasional cells labeled in INL and no cone labeling
Cytochrome oxidase	Good staining of rod and cone IS	Reasonable preservation of normal staining pattern, with some reduced intensity	Moderate staining pattern, with cone IS staining better than rod IS	Poor staining, essentially restricted to cone IS
Synaptophysin	Good, tight OPL and IPL with normal synaptic staining	IPL relatively normal; OPL architecture good with some axon retraction and redistribution to cell bodies of ONL	IPL still reasonable, OPL appearance expanded due to retraction/ extension of axons; some rod terminal dropout	IPL staining weaker; OPL thin due to rod terminal dropout with clustering of surviving rod terminals around cone pedicles

Total score for the listed antibodies is 6–18. Intermediate filament staining (GFAP and Vimentin): +1, upregulation to OLM; +1, focal breach of ILM/OLM; +1, multilayered component (ERM or SRM); maximum, +5 for GFAP and +5 for vimentin, giving a theoretical maximum total of +10; minimum is +2 in total, as GFAP and vimentin are always upregulated to the OLM. Other scores: +1, significant ILM wrinkling; +1, rod axon extension. This system gives a combined score between 8 and 30 as a summary statistic of intra- and periretinal pathology, based on the panel of antibodies used in this study.

TABLE 3. Prevalence of Immunohistochemical and Morphological Observations

	Specimens (*n*)
Rod photoreceptors with OS and IS	
<25% total rod PR count	5
25–50% total rod PR count	3
50–75% total rod PR count	3
>75% total rod PR count	5
Rod axon extension	16
Extraretinal gliosis	
Epiretinal membrane formation	9
Subretinal gliosis	11
PR immunostaining (anti-opsin)	
Rods	16
M/L cones	14
S cones	10

$n = 16$. Staining for rod photoreceptors (PR) was present in all sections and allowed a simple assessment of viability based on the proportion of positive cells possessing morphologically discernable outer (OS) and inner segments (IS).

shows that the incidence of PVR remains between 5.1% and 11.7% after primary RD surgery.[10] Surgical success, defined as anatomic retinal reattachment, may be achieved in as many as 90% of initial PVR cases and in 86% involving repeat procedures, although visual recovery is often disappointing, with only 19% of eyes achieving 20/100 vision or better after one operation, and in only 11%, should more than one procedure be required.[13,14]

Our present study provides new information about the behavior of intrinsic glial and neuronal components of full-thickness human neurosensory retina after RD complicated by PVR. There are disadvantages of studying human material at an advanced stage of disease. Differences in the etiology of RD, number of procedures performed, and uncertainty about the precise duration of RD create inherent variability in the experimental substrate. Photoreceptor cell death and other pathologic changes are also likely to vary with the height of RD.[15–17] Indeed, best corrected visual acuity has been shown to be significantly worse with increasing height of RD at the central fovea, as measured by optical coherence tomography.[18]

Our specimens are obtained at the end stage of a disease process in which retinal cells have been exposed to a biologically hostile environment for a variable but usually protracted period. The frequency of reproliferation[13,14] may reflect that, once such hostility has initiated cellular proliferation leading to PVR, cells remain primed. Removal of full-thickness retina at relaxing surgery for PVR may have the advantage of removing some of those primed intraretinal cells, such as Müller glia or astrocytes, that may otherwise contribute to recurrent PVR, though this still occurs to a clinically detectable level in 20% to 50% of eyes with extensive retinectomies.[19,20] This surgical approach is really the only source of full-thickness retinal and periretinal tissue specimens essential for a study of this kind.

Müller Glia and Periretinal Membranes

An increase in intermediate filaments throughout the entire Müller cell was seen in all specimens, as demonstrated by anti-GFAP and anti-vimentin labeling, consistent with previous observations in human tissue.[21] In experimental primate RD, this increase was observed after 7 days.[22] Using more sensitive detection systems in a feline model of RD, the process can be identified as beginning within a day of detachment, and by 3 days, intermediate filament containing Müller cell processes can occasionally be seen in the subretinal space at focal breaches of the OLM.[23,24] This Müller cell outgrowth is associated with cone photoreceptors in the cat[25] and possibly also in human RD (Fig. 4D). Experimentally, Müller cell proliferation is at its maximum at 3 to 4 days[26] and then continues at a slower rate for weeks to months.[27] The purpose of this injury response may be mechanical, to stabilize neural tissue faced with dynamic alterations in surface forces.

Data from experimental detachment suggest that some Müller cell nuclei migrate into the ONL or subretinal space within a few days of detachment. Hypertrophy and proliferation of these cells may interfere with OS regeneration on reattachment and adversely affect visual outcome.[15] Expansion of lateral processes from reactive Müller cells may also interfere with re-establishment of intraretinal synaptic connections on reattachment, as occurs with astrocytic scars in the central nervous system.[28] The distribution and level of amino acid transmitters and receptors also changes in detached retina, presumably influenced by altered glycemic status and tissue oxygen levels.[29–31] There is evidence to suggest that some of these changes may be ameliorated by elevating the partial pressure of inspired oxygen, alluding to a possible hypoxic mechanism behind some of the changes in glial morphology we have observed.[17,32]

Wrinkling of the ILM was a consistent feature, signifying incipient contraction in the region of Müller cell foot processes, and parallels observations in experimental RDs produced in owl monkey eyes.[33] In our study, this was observed even in the absence of ERM formation and is thus likely to be an early feature of detachment retinopathy, accompanying the expansion that occurs in Müller cell volume at the expense of degeneration in non-glial cell populations.

Hypertrophy and migration of Müller cells, and possibly astrocytes, onto the surfaces of detached retina was demonstrated in several of the specimens, varying from focal gliosis to multiple layers of glial cell processes. Previous experimental studies employing tritiated thymidine incorporation have demonstrated that these cells are proliferating on both retinal surfaces and are not merely migrating from the retina.[33,34] Contraction of "complex" ERMs has been attributed to the presence of fibroblastic cells that may be derived from RPE cells that have transdifferentiated from an epithelial to a mesenchymal phenotype.[35,36] We found some cytokeratin-positive pigment epithelial-derived cells in periretinal membranes in these specimens (data not shown).

The frequency with which ERMs were encountered in our study (9/16 specimens) could have been influenced by attempts at membrane peeling at the time of relaxing surgery, previous membrane-peeling surgery, or sampling variability during the processing of thick sections for immunohistochemistry by laser scanning confocal microscopy. Small membrane components attached to the retina by glial pegs, noted in previous studies,[37] may thus represent incipient new membranes or residual components from prior peeling surgery. In many cases, where the retinal origin of epiretinal gliosis could be discerned, we found it to be adjacent to large vessels in the inner retina, as have other investigators.[38] This may be because the ILM overlying these vessels is thinner and easier to breach or has already been partially ruptured at the time of posterior vitreous detachment, given that perivascular adhesions are generally stronger than adhesion to adjacent neural retina.[39,40] Alternatively, it is possible that alterations in the blood–retinal barrier occurs in these regions, with transmigration of cells and release of soluble factors from the vasculature, which incite glial reactivity locally.

There appears to be some species variation in the avidity with which Müller cells breach the OLM and enter the subretinal space. Focal breaches appear by 3 days in a feline model of RD, progressing to more confluent subretinal plaques by day 7.[23] After 28 days, all animals have large areas of subretinal

gliosis and corresponding degeneration of subjacent photoreceptors.[24] Subretinal gliosis was reported in 16 of 37 eyes in a series by Lewis and Aaberg.[13] Our results are broadly similar (11/16), though most of the pathology encountered consisted of focal breaches of the OLM, with relatively few (2/16) specimens demonstrating confluent subretinal gliosis. When this did occur, there was the expected reduction in the number and integrity of adjacent photoreceptors, some of which had nuclei that were drawn into the gliotic complex (Figs. 4E, 4F).

Photoreceptors

Photoreceptor cell death has been shown to occur mainly by apoptosis in human[41] and experimental RD.[6,39,42] In feline RD, the peak of TUNEL-positive cells is observed at day 3, declining rapidly thereafter,[6] and it is thus not surprising that, in the chronically detached human tissue that we studied, there was little evidence of TUNEL labeling.

Redistribution of opsin protein in photoreceptors agrees with observations in experimental detachment and retinal degeneration.[43–45] In normal retina, opsin is essentially restricted to the OS, though low levels may be found in the plasma membrane of other cell compartments.[46] After experimental RD, opsin presumably continues to be synthesized, transported to the OS of surviving photoreceptors, and inserted into disc membranes. There is immunohistochemical evidence of opsin protein redistribution to the plasma membrane associated with the IS, cell bodies, axons, and synaptic terminals,[46] perhaps due to the inability of cells to form normal OS, so that newly synthesized opsin is inserted into the plasma membrane. Our analysis of human RD tissue corroborates these findings, with increasing opsin protein redistribution to the plasma membrane of more proximal cell compartments after degeneration of the OS. Experimental retinal reattachment halts the redistribution of rod opsin,[9] and intravitreal treatment with brain-derived neurotrophic factor or hyperoxia reduces it in a feline model.[47,48]

Rod opsin was detected in all specimens by immunohistochemistry, M/L-cone opsin in 14 of 16 and S-cone opsin in 10 of 16. This apparent hierarchy of sensitivity to immunohistochemical detection parallels observations in experimental detachment, where anti-rod opsin staining is detectable after months of detachment, but anti-M/L-cone opsin staining seldom persists after 7 days, with anti-S-cone opsin staining detectable for even shorter periods.[49,50] Rapid loss of currently available cone markers after experimental RD has been one limiting factor in elucidating survival mechanisms in this functionally critical cell population. An additional consideration in this study is that we analyzed rod-dominant pre-equatorial retina, which would be expected to have a lower number of immunohistochemically detectable cones than more central retina.

Neural Plasticity

Remodeling of first-, second- and third-order neurons after RD complicated by PVR suggests that the retina may still be capable of mounting a regenerative response. Demonstration of anti-cytochrome oxidase labeling in the IS of photoreceptors and large cell bodies of higher order neurons certainly suggests that the metabolic capacity for regeneration is retained even after prolonged RD.

First-Order Neurons. Ultrastructural studies have demonstrated that retraction of rod synaptic terminals begins rapidly (within 1 day) of experimental RD.[15] Cones do not retract, but their terminals flatten and change shape, losing their complex synaptic invaginations.[5] In humans with secondary RD, there is a reduction in the number of photoreceptor synaptic terminals with time,[51] and our data suggest that as photoreceptor terminals are lost in the OPL, surviving rod terminals tend to cluster around viable cone pedicles (Fig. 2P, arrow and inset; Fig. 3C, arrows), supporting the theory that rods may produce a diffusible signal necessary to maintain cone viability, or that in areas of massive rod breakdown, cones are exposed to a potentially lethal microenvironment.[52,53] Alternatively, cones may produce rod survival factors.

Rod axon extension past the OPL and toward the inner retina was demonstrated in virtually all specimens. Where not seen (2/16), the retina was extremely degenerated, suggesting that rod photoreceptors may be too injured to mount neurite extension or that the level of opsin protein present in extending neurites is below the threshold of detection when these methods are used. In some of the specimens that demonstrated neurite extension, double labeling with ant-rod opsin and anti-synaptophysin revealed that the extending neurites contained synaptic vesicle protein in their varicosities. It appears that the machinery for functional synapse reformation is retained even in prolonged RD, and may thus be amenable to manipulation once we understand these processes more fully. Rod neurite sprouting has been observed in other experimental and clinical situations where the OS degenerates, including human retinitis pigmentosa[54,55] and autosomal dominant feline rod-cone dysplasia.[56] Compensatory synaptic growth in the rod terminals may have important implications for the maintenance of visual sensitivity in the diseased or aging retina.[57]

Second-Order Neurons. Remodeling in second-order neurons was demonstrated in horizontal and rod bipolar cells by labeling with anti-calbindin D and anti-PKC, respectively (Figs. 5C–E). This parallels observations in experimental feline RD, in which fine rod bipolar cell and horizontal cell processes extend past the normal layer of rod terminals into the ONL within days.[5] Horizontal cell neurite sprouting has also been demonstrated in the RCS rat[58] and in human retinitis pigmentosa.[54]

As rod photoreceptor terminals retract toward cell bodies in the ONL, demonstrated by anti-synaptophysin labeling (Fig. 2O, arrow), it appears that dendrites from surviving second-order neurons attempt to maintain functional and trophic contact by extending beyond the OPL into the ONL. This extension is accompanied by a reduction in the number of cells staining positive for anti-calbindin D in the INL (Figs. 2J–L) and disorganization among the normally well-ordered array of rod bipolar cell bodies (Fig. 5D). The molecular stimulus for neurite outgrowth in these circumstances is not known but may involve basic fibroblast growth factor released from retracting photoreceptor terminals or other neurotrophic agents.[22,59–61]

Third-Order Neurons. Increase in anti-neurofilament labeling in ganglion cell bodies after RD (Fig. 5G) also parallels experimental observations. In the feline model, increased labeling is also seen in horizontal cell bodies and processes, though human horizontal cells are phenotypically different and do not demonstrate anti-neurofilament labeling.[62] Larger ganglion cells appeared to sprout neurites directly from somata, but also from axon collaterals. Such morphologic plasticity on injury reflects the transient exuberance of dendritic and somatic spines seen during the neuronal development of this class of cells.[63–65] Where ERMs were detected, these processes were seen to extend into the glial tissue composing the membrane (Fig. 5F), and were also consistent features in epiretinal tissue peeled in separate operations (Fig. 5H). Neural elements have also been detected in epiretinal glial tissue by other investigators (Paul Hiscott, personal communication, 2001).

Growth-associated protein-43 (GAP-43) has been termed a "growth" or "plasticity" protein, because it is expressed at high levels in neuronal growth cones during development and during axonal regeneration.[66–68] This protein is abundant during development but absent in normal adult retina. Our detection of injury-induced re-expression of this developmentally regu-

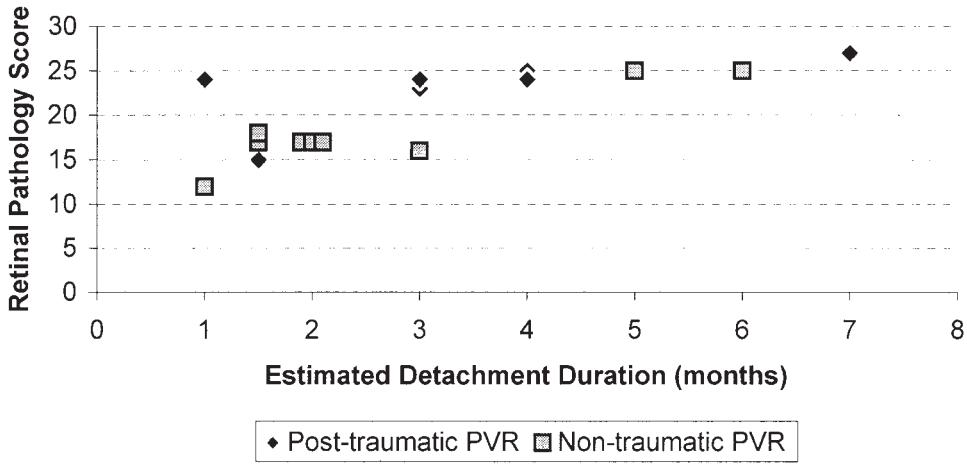

FIGURE 6. Graph of retinal pathology scores as derived in Table 2 against total estimated duration of RD in months. Traumatic PVR cases are distinguished from those not involving trauma. The majority (6/8) of high-scoring specimens (>20) were from cases of traumatic PVR. Of those scoring less than 20, five of six had cumulative detachment durations of ≤2 months.

lated protein in ganglion cells implies plasticity and regenerative capacity in a central nervous system neuron. This agrees with observations in experimental feline RD,[69] and is a feature of axon injury models.[8]

Glial–Neuronal Interactions

There appears to be an association with reactive glia in the neural remodeling events described, with extending neurites preferring to course along a hypertrophied Müller cell trunk (Figs. 2D, 5A). These glial cells undergo significant cellular and molecular changes that begin rapidly after RD.[70] Some of these processes may be related to wound healing and tissue repair, whereas others may subserve a protective function. Müller cells express high-affinity glutamate uptake systems that protect neurons from excitotoxic damage.[71] Not only do they buffer the ionic microenvironment conducive to neuronal function,[72] but they also have extensive energy reserves that may protect neurons at times of retinal ischemia.[73]

There is convincing evidence to suggest that the photoreceptor rescuing effects of some neurotrophic factors are exerted through Müller cells and possibly some other nonphotoreceptor cells of the inner retina. Wahlin et al.[74] have demonstrated that brain-derived neurotrophic factor (BDNF), ciliary neurotrophic factor (CNTF), and fibroblast growth factor-2 (FGF-2) activate intracellular signaling pathways in Müller cells, accompanied by increased staining for GFAP, but not in photoreceptors. Müller cells may also be an endogenous source of various survival factors for retinal neurons[75–77] and may play a role in the phagocytosis of cellular debris after retinal injury.[78]

Rather than just creating physical barriers to neurite growth, our data suggest that reactive gliosis may facilitate neurite sprouting under some circumstances and act as a preferred scaffold for regeneration. This has been demonstrated for in vitro neurite extension by rod photoreceptor cells,[79] and in vitro analysis of retinal ganglion cell neurite outgrowth on Müller cells has implicated neural cell adhesion molecules in this process.[80] Characterizing the molecular bases of these interactions may allow the exploitation of guidance cues in future therapies and improve *functional* outcome in a surgical arena where macroanatomic success is already within our grasp.

Use of the Retinal Pathology Scoring System

Our analysis of full-thickness retinectomy specimens in conjunction with normal human retinas enabled us to identify precisely the cellular and subcellular changes associated with human RD complicated by PVR. Grading the severity of change in retinal cell biology after detachment is dependent on reliable immunohistochemical methods and may thus change as techniques develop and new antibodies emerge. However, despite the complexity of pathology encountered in a given specimen, the pattern of change from normal for each primary label was characteristic. A well-characterized panel of antibodies was used to derive a retinal pathology score, as summarized in Table 2, which takes into account glial and neuronal components of the retina, metabolic potential and synaptic connectivity.

Figure 6 illustrates the retinal pathology score for each specimen, as a function of estimated cumulative duration of detachment. The total score, as derived in Table 2, gives a value between 6 and 30. There is an association between more advanced degeneration (higher scores) and longer detachment duration. In experimental feline RD, the severity of morphologic change is also strongly associated with the duration of RD,[15,16,81] and several clinical studies have suggested that final visual acuity is attributable largely to the duration of macular detachment.[60,82–84]

Traumatic PVR also tended to have higher pathology scores and is clinically associated with poorer visual outcome.[85] If we take 20 as an arbitrary score representing significant degeneration, we can see that six of eight specimens with scores higher than 20 were traumatic cases. In addition, if we look at detachment duration, of those cases with scores higher than 20, only one of eight had incurred less than 2 months of cumulative RD. This case involved traumatic PVR with penetrating injury, dense vitreous hemorrhage, and iris prolapse. There was no association between the retinal pathology score and the use of silicone oil at any time before the surgery during which the specimen was obtained (data not shown).

The correlations described appear to validate the simple scoring system we have used in describing the range of pathology encountered in human RD complicated by PVR. In general, there was an association between higher aggregate scores for intermediate filament staining and a high overall score, suggesting that periretinal glial proliferation is associated with more degenerative neural intraretinal changes. Our analysis did not specifically take into account remodeling events in second- and third-order neurons, but as these phenomena seemed to be relatively consistent observations in the material studied, we elected to score rod axon extension as a representative marker for neuronal remodeling. Rod axon extension has been given a point as "pathology" even though it may represent an attempt at recovery. This is because we have only seen this phenomenon in the context of OS degeneration, and thus, whereas the ability to mount such a response may suggest the photorecep-

tors are amenable to rescue, its observation is a testament to antecedent retinal injury.

Scoring the retinal cell biology of human RD complicated by PVR in this manner formalizes our approach to assessing structural changes in small samples of retinal tissue and establishes a systematic database of intraretinal and periretinal pathology in complex human RD. This may be relevant in clinical studies in which retinal biopsy specimens are available for morphologic analysis and provide an albeit semiquantitative method of comparison between specimens that may have statistical relevance. The information we present also allows critical appraisal of experimental models as analogues for studying pathogenesis and intervention in PVR.

Conclusions

In general, the cellular and subcellular changes we studied in human RD complicated by PVR varied consistently with increasing severity of retinal degeneration. A proposed scoring system may be useful in future clinical trial work. In most cases, the structural motifs necessary for initiating recovery were still present, even in the most advanced degeneration, though in various states of disarray. The morphologic changes observed in retinectomy material would have profound effects on visual recovery if they occurred as part of macular detachment. Many patients describe improvement in some visual parameters during the year after macular reattachment.[86] Visual acuity can continue to improve for several years, particularly in young patients without significant myopia in whom the duration of macular detachment has been less than 30 days,[87] perhaps due in part to a gradual increase in OS length,[88] but the effect of reattachment on disordered retinal circuitry has not been established.

Analysis of growth factors and cytokines in periretinal membranes, subretinal fluid, and vitreous from patients with PVR suggests that this phenomenon bears the hallmarks of an aberrant or exaggerated wound-healing response in detached retina.[89–91] The reliability with which neural elements are retained and the observation that retinal strata are occasionally well preserved despite periretinal membrane formation suggest that some cellular and molecular sequelae of RD with PVR may serve a protective function. In cases with poor visual outcome lacking gross pathology such as epiretinal proliferation or subretinal gliosis, the surgeon should suspect intraretinal pathology in neuronal and glial components of the reattached retina. Some of these may be amenable to reversal, with corresponding improvement in functional indices. The study of human tissue from end-stage disease allows us to comment only on the likelihood that such reparation is possible. Establishing reversibility depends ultimately on correlating the specific cellular changes described herein to their functional consequences in experimental systems that exhibit analogous changes and are amenable to the sophisticated surgical interventions used in clinical practice.[9,87,92]

Preventing photoreceptor deconstruction is only the first goal in effective visual rehabilitation after RD. Active remodeling of neural and glial retinal components occurs in complex molecular association, the characterization of which ultimately holds the key to functionally successful surgery.

Acknowledgments

The authors thank Zoe Adams for editorial support; the nursing and technical staff in the Department of Vitreoretinal Surgery, Moorfields Eye Hospital, in particular, Staff Nurse Donna Boyle and Graham Nunn for their help in obtaining the specimens used in this study; and the surgeons and patients of Moorfields Eye Hospital without whose cooperation this work would not have been possible.

References

1. Machemer R, Aaberg TM, Freeman HM, Irvine AR, Lean JS, Michels RM. An updated classification of retinal detachment with proliferative vitreoretinopathy. *Am J Ophthalmol.* 1991;112:159–165.
2. Weller M, Wiedemann P, Heimann K. Proliferative vitreoretinopathy: is it anything more than wound healing at the wrong place? *Int Ophthalmol*. 1990;14:105–117.
3. Mietz H, Kirchhof B, Heimann K. Anterior proliferative vitreoretinopathy in trauma and complicated retinal detachment: a histopathologic study. *Ger J Ophthalmol*. 1994;3:15–18.
4. Erickson PA, Fisher SK, Guerin CJ, Anderson DH, Kaska DD. Glial fibrillary acidic protein increases in Müller cells after retinal detachment. *Exp Eye Res*. 1987;44:37–48.
5. Lewis GP, Linberg KA, Fisher SK. Neurite outgrowth from bipolar and horizontal cells after experimental retinal detachment. *Invest Ophthalmol Vis Sci*. 1998;39:424–434.
6. Cook B, Lewis GP, Fisher SK, Adler R. Apoptotic photoreceptor degeneration in experimental retinal detachment. *Invest Ophthalmol Vis Sci*. 1995;36:990–996.
7. Pow DV, Robinson SR. Glutamate in some retinal neurons is derived solely from glia. *Neuroscience*. 1994;60:355–366.
8. Meyer RL, Miotke JA, Benowitz LI. Injury induced expression of growth-associated protein-43 in adult mouse retinal ganglion cells in vitro. *Neuroscience*. 1994;63:591–602.
9. Lewis GP, Charteris DG, Sethi CS, Leitner WP, Linberg KA, Fisher SK. The ability of rapid retinal reattachment to stop or reverse the cellular and molecular events initiated by detachment. *Invest Ophthalmol Vis Sci*. 2002;43:2412–2420.
10. Charteris DG, Sethi CS, Lewis GP, Fisher SK. Proliferative vitreoretinopathy: developments in adjunctive treatment and retinal pathology. *Eye*. 2002;16:369–374.
11. Asaria RH, Kon CH, Bunce C, et al. Adjuvant 5-fluorouracil and heparin prevents proliferative vitreoretinopathy: results from a randomized, double-blind, controlled clinical trial. *Ophthalmology*. 2001;108:1179–1183.
12. Wiedemann P, Hilgers RD, Bauer P, Heimann K. Adjunctive daunorubicin in the treatment of proliferative vitreoretinopathy: results of a multicenter clinical trial. Daunomycin Study Group. *Am J Ophthalmol.* 1998;126:550–559.
13. Lewis H, Aaberg TM. Causes of failure after repeat vitreoretinal surgery for recurrent proliferative vitreoretinopathy. *Am J Ophthalmol.* 1991;111:15–19.
14. Lewis H, Aaberg TM, Abrams GW. Causes of failure after initial vitreoretinal surgery for severe proliferative vitreoretinopathy. *Am J Ophthalmol.* 1991;111:8–14.
15. Erickson PA, Fisher SK, Anderson DH, Stern WH, Borgula GA. Retinal detachment in the cat: the outer nuclear and outer plexiform layers. *Invest Ophthalmol Vis Sci*. 1983;24:927–942.
16. Anderson DH, Stern WH, Fisher SK, Erickson PA, Borgula GA. Retinal detachment in the cat: the pigment epithelial–photoreceptor interface. *Invest Ophthalmol Vis Sci*. 1983;24:906–926.
17. Sakai T, Lewis GP, Linberg KA, Fisher SK. The ability of hyperoxia to limit the effects of experimental detachment in cone-dominated retina. *Invest Ophthalmol Vis Sci*. 2001;42:3264–3273.
18. Hagimura N, Suto K, Iida T, Kishi S. Optical coherence tomography of the neurosensory retina in rhegmatogenous retinal detachment. *Am J Ophthalmol.* 2000;129:186–190.
19. Federman JL, Eagle RC Jr. Extensive peripheral retinectomy combined with posterior 360 degrees retinotomy for retinal reattachment in advanced proliferative vitreoretinopathy cases. *Ophthalmology*. 1990;97:1305–1320.
20. Alturki WA, Peyman GA, Paris CL, Blinder KJ, Desai UR, Nelson NC Jr. Posterior relaxing retinotomies: analysis of anatomic and visual results. *Ophthalmic Surg*. 1992;23:685–688.
21. Okada M, Matsumura M, Ogino N, Honda Y. Müller cells in detached human retina express glial fibrillary acidic protein and vimentin. *Graefes Arch Clin Exp Ophthalmol*. 1990;228:467–474.

22. Guerin CJ, Anderson DH, Fisher SK. Changes in intermediate filament immunolabeling occur in response to retinal detachment and reattachment in primates (published correction appears in *Invest Ophthalmol Vis Sci.* 1990;31:2360). *Invest Ophthalmol Vis Sci*. 1990;31:1474–1482.
23. Lewis GP, Guerin CJ, Anderson DH, Matsumoto B, Fisher SK. Rapid changes in the expression of glial cell proteins caused by experimental retinal detachment. *Am J Ophthalmol.* 1994;118:368–376.
24. Lewis GP, Matsumoto B, Fisher SK. Changes in the organization and expression of cytoskeletal proteins during retinal degeneration induced by retinal detachment. *Invest Ophthalmol Vis Sci*. 1995;36:2404–2416.
25. Lewis GP, Fisher SK. Müller cell outgrowth after retinal detachment: association with cone photoreceptors. *Invest Ophthalmol Vis Sci*. 2000;41:1542–1545.
26. Fisher SK, Erickson PA, Lewis GP, Anderson DH. Intraretinal proliferation induced by retinal detachment. *Invest Ophthalmol Vis Sci*. 1991;32:1739–1748.
27. Geller SF, Lewis GP, Anderson DH, Fisher SK. Use of the MIB-1 antibody for detecting proliferating cells in the retina. *Invest Ophthalmol Vis Sci*. 1995;36:737–744.
28. Dusart I, Marty S, Peschanski M. Glial changes following an excitotoxic lesion in the CNS. II. Astrocytes. *Neuroscience*. 1991;45: 541–549.
29. Fisher SK, Anderson DH. Cellular effects of retinal detachment on the neural retina and the retinal pigment epithelium. In: Ryan S, ed. *Retina.* 3rd ed. St. Louis: Mosby; 2001:1961–1986.
30. Marc RE, Murry RF, Fisher SK, Linberg KA, Lewis GP. Amino acid signatures in the detached cat retina. *Invest Ophthalmol Vis Sci*. 1998;39:1694–1702.
31. Marc RE, Murry RF, Fisher SK, Linberg KA, Lewis GP, Kalloniatis M. Amino acid signatures in the normal cat retina. *Invest Ophthalmol Vis Sci*. 1998;39:1685–1693.
32. Lewis G, Mervin K, Valter K, et al. Limiting the proliferation and reactivity of retinal Müller cells during experimental retinal detachment: the value of oxygen supplementation. *Am J Ophthalmol.* 1999;128:165–172.
33. Laqua H, Machemer R. Glial cell proliferation in retinal detachment (massive periretinal proliferation). *Am J Ophthalmol.* 1975;80: 602–618.
34. Erickson PA, Guerin CJ, Fisher SK. Tritiated uridine labeling of the retina: changes after retinal detachment. *Exp Eye Res*. 1990;51: 153–158.
35. Hiscott P, Sheridan C, Magee RM, Grierson I. Matrix and the retinal pigment epithelium in proliferative retinal disease. *Prog Retin Eye Res*. 1999;18:167–190.
36. Grisanti S, Guidry C. Transdifferentiation of retinal pigment epithelial cells from epithelial to mesenchymal phenotype. *Invest Ophthalmol Vis Sci*. 1995;36:391–405.
37. McLeod D, Hiscott PS, Grierson I. Age-related cellular proliferation at the vitreoretinal juncture. *Eye*. 1987;1:263–281.
38. Daicker B, Guggenheim R, Gywat L. Findings on the retinal surface by scanning electron microscopy. III. Epivascular glial clusters (in German). *Albrecht Von Graefes Arch Klin Exp Ophthalmol*. 1977; 204:31–37.
39. Kishi S, Numaga T, Yoneya S, Yamazaki S. Epivascular glia and paravascular holes in normal human retina. *Graefes Arch Clin Exp Ophthalmol*. 1986;224:124–130.
40. Foos RY. Vitreoretinal juncture over retinal vessels. *Albrecht Von Graefes Arch Klin Exp Ophthalmol*. 1977;204:223–234.
41. Chang CJ, Lai WW, Edward DP, Tso MO. Apoptotic photoreceptor cell death after traumatic retinal detachment in humans. *Arch Ophthalmol*. 1995;113:880–886.
42. Hisatomi T, Sakamoto T, Goto Y, et al. Critical role of photoreceptor apoptosis in functional damage after retinal detachment. *Curr Eye Res*. 2002;24:161–172.
43. Fariss RN, Molday RS, Fisher SK, Matsumoto B. Evidence from normal and degenerating photoreceptors that two outer segment integral membrane proteins have separate transport pathways. *J Comp Neurol*. 1997;387:148–156.
44. Nir I, Papermaster DS. Immunocytochemical localization of opsin in the inner segment and ciliary plasma membrane of photoreceptors in retinas of rds mutant mice. *Invest Ophthalmol Vis Sci*. 1986;27:836–840.
45. Usukura J, Bok D. Changes in the localization and content of opsin during retinal development in the rds mutant mouse: immunocytochemistry and immunoassay. *Exp Eye Res*. 1987;45:501–515.
46. Lewis GP, Erickson PA, Anderson DH, Fisher SK. Opsin distribution and protein incorporation in photoreceptors after experimental retinal detachment. *Exp Eye Res*. 1991;53:629–640.
47. Mervin K, Valter K, Maslim J, Lewis G, Fisher S, Stone J. Limiting photoreceptor death and deconstruction during experimental retinal detachment: the value of oxygen supplementation. *Am J Ophthalmol.* 1999;128:155–164.
48. Lewis GP, Linberg KA, Geller SF, Guerin CJ, Fisher SK. Effects of the neurotrophin brain-derived neurotrophic factor in an experimental model of retinal detachment. *Invest Ophthalmol Vis Sci*. 1999;40:1530–1544.
49. Rex TS, Fariss RN, Lewis GP, Linberg KA, Sokal I, Fisher SK. A survey of molecular expression by photoreceptors after experimental retinal detachment. *Invest Ophthalmol Vis Sci*. 2002;43: 1234–1247.
50. Linberg KA, Lewis GP, Shaaw C, Rex TS, Fisher SK. Distribution of S- and M-cones in normal and experimentally detached cat retina. *J Comp Neurol*. 2001;430:343–356.
51. Kroll AJ. Secondary retinal detachment: electron microscopy of retina and pigment epithelium. *Am J Ophthalmol.* 1969;68:223–237.
52. Mohand-Said S, Hicks D, Leveillard T, Picaud S, Porto F, Sahel JA. Rod-cone interactions: developmental and clinical significance. *Prog Retin Eye Res*. 2001;20:451–467.
53. Hicks D, Sahel J. The implications of rod-dependent cone survival for basic and clinical research. *Invest Ophthalmol Vis Sci*. 1999; 40:3071–3074.
54. Fariss RN, Li ZY, Milam AH. Abnormalities in rod photoreceptors, amacrine cells, and horizontal cells in human retinas with retinitis pigmentosa. *Am J Ophthalmol.* 2000;129:215–223.
55. Li ZY, Kljavin IJ, Milam AH. Rod photoreceptor neurite sprouting in retinitis pigmentosa. *J Neurosci*. 1995;15:5429–5438.
56. Chong NH, Alexander RA, Barnett KC, Bird AC, Luthert PJ. An immunohistochemical study of an autosomal dominant feline rod/cone dysplasia (Rdy cats). *Exp Eye Res*. 1999;68:51–57.
57. Sanyal S, Hawkins RK, Jansen HG, Zeilmaker GH. Compensatory synaptic growth in the rod terminals as a sequel to partial photoreceptor cell loss in the retina of chimaeric mice. *Development*. 1992;114:797–803.
58. Chu Y, Humphrey MF, Constable IJ. Horizontal cells of the normal and dystrophic rat retina: a wholemount study using immunolabelling for the 28-kDa calcium-binding protein. *Exp Eye Res*. 1993; 57:141–148.
59. Wen R, Song Y, Cheng T, et al. Injury-induced upregulation of bFGF and CNTF mRNAs in the rat retina. *J Neurosci*. 1995;15: 7377–7385.
60. Li ZY, Chang JH, Milam AH. A gradient of basic fibroblast growth factor in rod photoreceptors in the normal human retina. *Vis Neurosci*. 1997;14:671–679.
61. Lewis GP, Fisher SK, Anderson DH. Fate of biotinylated basic fibroblast growth factor in the retina following intravitreal injection. *Exp Eye Res*. 1996;62:309–324.
62. Kivela T, Tarkkanen A, Virtanen I. Intermediate filaments in the human retina and retinoblastoma: an immunohistochemical study of vimentin, glial fibrillary acidic protein, and neurofilaments. *Invest Ophthalmol Vis Sci*. 1986;27:1075–1084.
63. Ramoa AS, Campbell G, Shatz CJ. Dendritic growth and remodeling of cat retinal ganglion cells during fetal and postnatal development. *J Neurosci*. 1988;8:4239–4261.
64. Lei JL, Lau KC, So KF, Cho EY, Tay D. Morphological plasticity of axotomized retinal ganglion cells following intravitreal transplantation of a peripheral nerve segment. *J Neurocytol*. 1995;24:497–506.
65. Eysel UT, Peichl L, Wassle H. Dendritic plasticity in the early postnatal feline retina: quantitative characteristics and sensitive period. *J Comp Neurol*. 1985;242:134–145.
66. Shen Y, Mani S, Donovan SL, Schwob JE, Meiri KF. Growth-associated protein-43 is required for commissural axon guidance in

the developing vertebrate nervous system. *J Neurosci*. 2002;22: 239–247.

67. Baekelandt V, Eysel UT, Orban GA, Vandesande F. Long-term effects of retinal lesions on growth-associated protein 43 (GAP-43) expression in the visual system of adult cats. *Neurosci Lett*. 1996; 208:113–116.
68. Kapfhammer JP, Christ F, Schwab ME. The expression of GAP-43 and synaptophysin in the developing rat retina. *Brain Res Dev Brain Res*. 1994;80:251–260.
69. Coblentz FE, Radeke MJ, Lewis GP, Fisher SK. Evidence that ganglion cells react to retinal detachment. *Exp Eye Res.* 2003;76:333–342.
70. Geller SF, Lewis GP, Fisher SK. FGFR1, signaling, and AP-1 expression after retinal detachment: reactive Müller and RPE cells. *Invest Ophthalmol Vis Sci*. 2001;42:1363–1369.
71. Heidinger V, Hicks D, Sahel J, Dreyfus H. Ability of retinal Müller glial cells to protect neurons against excitotoxicity in vitro depends upon maturation and neuron-glial interactions. *Glia*. 1999; 25:229–339.
72. Newman EA, Zahs KR. Modulation of neuronal activity by glial cells in the retina. *J Neurosci*. 1998;18:4022–4028.
73. Ripps H, Witkovsky P. Neuron-glial interaction in the brain and retina. *Prog Retin Eye Res*. 1985;4:181–219.
74. Wahlin KJ, Campochiaro PA, Zack DJ, Adler R. Neurotrophic factors cause activation of intracellular signaling pathways in Müller cells and other cells of the inner retina, but not photoreceptors. *Invest Ophthalmol Vis Sci*. 2000;41:927–936.
75. Honjo M, Tanihara H, Kido N, Inatani M, Okazaki K, Honda Y. Expression of ciliary neurotrophic factor activated by retinal Müller cells in eyes with NMDA- and kainic acid-induced neuronal death. *Invest Ophthalmol Vis Sci*. 2000;41:552–560.
76. Oku H, Ikeda T, Honma Y, et al. Gene expression of neurotrophins and their high-affinity Trk receptors in cultured human Müller cells. *Ophthalmic Res*. 2002;34:38–42.
77. Frasson M, Picaud S, Leveillard T, et al. Glial cell line-derived neurotrophic factor induces histologic and functional protection of rod photoreceptors in the rd/rd mouse. *Invest Ophthalmol Vis Sci*. 1999;40:2724–2734.
78. Francke M, Makarov F, Kacza J, et al. Retinal pigment epithelium melanin granules are phagocytosed by Müller glial cells in experimental retinal detachment. *J Neurocytol*. 2001;30:131–136.
79. Kljavin IJ, Reh TA. Müller cells are a preferred substrate for in vitro neurite extension by rod photoreceptor cells. *J Neurosci*. 1991; 11:2985–2994.
80. Drazba J, Lemmon V. The role of cell adhesion molecules in neurite outgrowth on Müller cells. *Dev Biol*. 1990;138:82–93.
81. Anderson DH, Guerin CJ, Erickson PA, Stern WH, Fisher SK. Morphological recovery in the reattached retina. *Invest Ophthalmol Vis Sci*. 1986;27:168–183.
82. Burton TC. Recovery of visual acuity after retinal detachment involving the macula. *Trans Am Ophthalmol Soc*. 1982;80:475–497.
83. Ross WH. Visual recovery after macula-off retinal detachment. *Eye*. 2002;16:440–6.
84. Hassan TS, Sarrafizadeh R, Ruby AJ, Garretson BR, Kuczynski B, Williams GA. The effect of duration of macular detachment on results after the scleral buckle repair of primary, macula-off retinal detachments. *Ophthalmology*. 2002;109:146–152.
85. Cardillo JA, Stout JT, LaBree L, et al. Post-traumatic proliferative vitreoretinopathy: the epidemiologic profile, onset, risk factors, and visual outcome. *Ophthalmology*. 1997;104:1166–1173.
86. Chisholm IA, McClure E, Foulds WS. Functional recovery of the retina after retinal detachment. *Trans Ophthalmol Soc UK*. 1975; 95:167–172.
87. Chang SD, Kim IT. Long-term visual recovery after scleral buckling procedure of rhegmatogenous retinal detachment involving the macula. *Kor J Ophthalmol*. 2000;14:20–26.
88. Guerin CJ, Lewis GP, Fisher SK, Anderson DH. Recovery of photoreceptor outer segment length and analysis of membrane assembly rates in regenerating primate photoreceptor outer segments. *Invest Ophthalmol Vis Sci*. 1993;34:175–183.
89. Miller B, Miller H, Patterson R, Ryan SJ. Retinal wound healing: cellular activity at the vitreoretinal interface. *Arch Ophthalmol*. 1986;104:281–285.
90. Charteris DG. Growth factors in proliferative vitreoretinopathy (Editorial). *Br J Ophthalmol*. 1998;82:106.
91. Kon CH, Occleston NL, Aylward GW, Khaw PT. Expression of vitreous cytokines in proliferative vitreoretinopathy: a prospective study. *Invest Ophthalmol Vis Sci*. 1999;40:705–712.
92. Lewis GP, Charteris DG, Sethi CS, Fisher SK. Animal models of retinal detachment and reattachment: identifying cellular events that may affect visual recovery. *Eye*. 2002;16:375–387.